Soft Matter

PAPER

View Article Online
View Journal | View Issue

Cite this: *Soft Matter*, 2018, **14**, 5811

Multiple particle tracking microrheology measured using bi-disperse probe diameters†

Matthew D. Wehrman,[a] Seth Lindberg[b] and Kelly M. Schultz *[a]

Multiple particle tracking microrheology (MPT) is a powerful tool for quantitatively characterizing rheological properties of soft matter. Traditionally, MPT uses a single particle size to characterize rheological properties. But in complex systems, MPT measurements with a single size particle can characterize distinct properties that are linked to the materials' length scale dependent structure. By varying the size of probes, MPT can measure the properties associated with different length scales within a material. We develop a technique to simultaneously track a bi-disperse population of probe particles. 0.5 and 2 μm particles are embedded in the same sample and these particle populations are tracked separately using a brightness-based squared radius of gyration, R_g^2. Bi-disperse MPT is validated by measuring the viscosity of glycerol samples at varying concentrations. Bi-disperse MPT measurements agree well with literature values. This technique then characterizes a homogeneous poly(ethylene glycol)-acrylate:poly(ethylene glycol)-dithiol gelation. The critical relaxation exponent and critical gelation time are consistent and agree with previous measurements using a single particle. Finally, degradation of a heterogeneous hydrogenated castor oil colloidal gel is characterized. The two particle sizes measure a different value of the critical relaxation exponent, indicating that they are probing different structures. Analysis of material heterogeneity shows measured heterogeneity is dependent on probe size indicating that each particle is measuring rheological evolution of a length scale dependent structure. Overall, bi-disperse MPT increases the amount of information gained in a single measurement, enabling more complete characterization of complex systems that range from consumer care products to biological materials.

Received 28th May 2018,
Accepted 27th June 2018

DOI: 10.1039/c8sm01098f

rsc.li/soft-matter-journal

1 Introduction

Multiple particle tracking microrheology (MPT) characterizes the rheological properties of soft materials by measuring the Brownian motion of micrometer sized probe particles to determine bulk properties.[1–15] The quantitative values determined by microrheology depend on the size of the probes relative to the feature size of the material.[13,16–18] Rheological properties of Newtonian fluids will be independent of particle size, but materials with complex microstructure can have different rheological properties based on the length scale being measured.[3,17,19–22] Here, we describe a MPT technique using bi-disperse probe particle sizes in a single sample. Bi-disperse particle sizes will measure feature sizes at different length scales, increasing the amount of information gained from each experiment, broadening the technique. This technique can maximize the information gained when characterizing high-value materials, by decreasing the amount of material and experiments, and heterogeneous scaffolds, where structural heterogeneities arise at different length scales and can be unique in each sample.

In MPT, fluorescently labeled probe particles are embedded into a sample and the Brownian motion of the particles is recorded using video microscopy. The particle positions are tracked and the Generalized Stokes–Einstein Relation (GSER) relates probe movement to rheological properties.[1–15] MPT measures material properties at equilibration and during phase transitions due to its unique characteristics. Specifically, when characterizing gel systems the sensitivity of MPT enables measurements of the weak incipient gel scaffolds at the gel point, with range of measurable elastic moduli of 10^{-3} to 4 Pa. The fast data acquisition, ~30 s, of MPT also enables measurements of evolving materials at a quasi-steady state.[8,14,23–28] In heterogeneous materials, the use of video microscopy to capture MPT data enables simultaneous characterization of the heterogeneous spatial microenvironment. These complimentary characteristics make MPT a powerful tool in the characterization of soft matter, but complete characterization of complex systems has been limited by the use of a single probe particle size.

[a] *Department of Chemical and Biomolecular Engineering, Lehigh University, Bethlehem, PA, USA. E-mail: kes513@lehigh.edu; Fax: +1-(610)-758-5057; Tel: +1-(610)-758-2012*

[b] *Process and Engineering Development, Procter & Gamble Co., West Chester, OH, USA*

† Electronic supplementary information (ESI) available: Additional experiments and sample analysis. See DOI: 10.1039/c8sm01098f

Previous studies have shown that changing probe particle size or surface chemistry can measure different properties and structures within a sample. Probe surface chemistry can be adjusted to reduce the interaction of probes with material, enabling measurement of bulk material properties.[29] Using both varying surface chemistry and probe particle size, MPT has been used to characterize oil-in-water emulsions. Plain polystyrene beads reside in the oil-rich phase while carboxylated beads reside in the oil-poor phase. In separate samples, probe size was varied to measure both the viscosity of single phases and the bulk properties of the emulsion.[20,21] Several studies have used multiple particle sizes in separate experiments to measure multiple length scales within a material.[17,19–22,30] Computational and experimental active microrheology experiments, where a probe particle is driven through a suspensions of bath particles, have investigated how changing probe size relative to the bath particle affects the flow-induced diffusion. They find that flow-induced diffusion is dependent on the strength of hydrodynamic interactions and that the difference in probe and bath particle size changes the relaxation of the microstructure.[30–32]

For MPT measurements using different size particles in separate experiments, the viscoelastic behavior of polymers above the overlap concentration, where there are increased polymeric interactions, show a dependence on probe particle size. When compared to MPT measurements below the overlap concentration, where there are minimal polymeric interactions, the change in particle size does not affect the measurements.[17] Multiple probe sizes in a single experiment have been previously used to measure biofilms.[33] Probes were added to the biofilm as it was growing and during growth probes of different sizes incorporated into the film in different areas. This enabled characterization of each part of the biofilm with a different particle size.[33] Our work builds off of this previous study to illustrate the utility of MPT with multiple particle sizes in a single sample and detail the tracking technique we use to measure each particle's microenvironment.

In this work, we describe bi-disperse MPT, MPT of two distinct particle sizes in a single sample. To illustrate this technique we use 0.5 and 2 μm fluorescently labeled polystyrene probes. We detail the method of tracking multiple particles by separating probes by their diameter using existing particle tracking algorithms. This is accomplished by leveraging the brightness-based squared radius of gyration, R_g^2, of the particle images. The ensemble-averaged mean-squared displacement (MSD) of each particle population, now separated by probe size, is calculated and used to determine the material properties of several systems. First, we validate the technique to ensure that each particle population is accurately measuring material properties. This is done by measuring the viscosity of a Newtonian fluid, glycerol, at varying concentrations. We find good agreement between the viscosity measured by each particle and literature values. A chain-growth polymer gelation, poly-(ethylene glycol) (PEG)-acrylate:PEG-dithiol, is then measured to illustrate that bi-disperse probe particles can accurately measure a homogeneous viscoelastic material. Finally, a hydrogenated castor oil (HCO) fibrous colloidal gel degradation is characterized to show the utility of the technique in measuring multiple length scales in a heterogeneous material. These experiments validate bi-disperse MPT and illustrate the advantages of measuring multiple length scales within a single sample. Overall, this technique broadens the available information gained from a single MPT measurement, which gives vital additional information to fully characterize materials ranging from consumer care products to biological materials.

2 Materials and methods

2.1 Materials

To show the usefulness of this technique, we have performed experiments on three known systems: glycerol,[34,35] a PEG-acrylate: PEG-dithiol cross-linked hydrogel[36] and an HCO colloidal gel.[6,7,37] In these experiments we show that both probe sizes accurately measure the material properties of Newtonian fluids and viscoelastic materials.

For all experiments two probe particle sizes are used, 0.5 μm and 2 μm probes. These particle sizes are chosen because they have different particle diameters enabling facile identification of each particle population. Additionally, the large probe particle size, 2 μm, was chosen because these probes do not settle over the time frame of our experiments. The particle used are 0.53 ± 0.01 μm and 1.83 ± 0.05 μm diameter carboxylated fluorescently labeled polystyrene probes (Polysciences, Inc.). Prior to bi-disperse MPT experiments, probes are washed 3× by alternating dilution and centrifugation. Final probe particle concentrations in each sample are 0.026% solids per volume and 0.1% solids per volume for 0.5 μm and 2 μm probes, respectively.

Initial experiments validated the measurements by each probe particle size using a concentration gradient of a viscous Newtonian fluid. In these experiments, glycerol (Alfa Aesar) is mixed with deionized water to precisely change the concentration between 0 and 40 wt%. For each glycerol concentration, probe particles are mixed into the sample at the final concentrations detailed above. The samples are then injected into a glass sample chamber, described previously, and sealed using UV curable adhesive (NOA-81, Norland Products Inc.).[36] The sample chamber is constructed of a glass slide with dimensions 25 × 75 × 1 mm (Thermo Fisher Scientific) with glass spacers (h = 0.16 mm) and a top coverslip with dimensions 22 × 22 × 0.16 mm (Thermo Fisher Scientific). For each sample, data are collected in three distinct places within the sample. For each concentration, three separate samples are characterized.

A photopolymerized polymer gel consisting of a four-arm star PEG end-terminated with acrylate (M_n = 20 000 g mol^{-1}, f = 4 where f is functionality, JenKem Technology) backbone and a linear PEG end-terminated with thiol (1500 g mol^{-1}, f = 2, JenKem Technology) cross-linker is characterized with bi-disperse MPT. Precursor solutions are made with 18 wt% PEG-acrylate and 3.8 wt% PEG-dithiol. The final ratio of thiol : acrylate is 1.4 : 1. 1.5 mM of lithium phenyl-2,4,6-trimethylbenzoylphosphinate (LAP), a photo-initiator, is added to the precursor solution.[38] Samples are injected into a sample chamber and sealed on both

sides with a two-part air cured epoxy (Gorilla Glue Company). Samples are exposed to ultraviolet (UV) light (output range 340–800 nm, 89 North, Inc.) for a specified amount of time to initiate the gelation reaction. After UV exposure, MPT measurements are collected. Data are collected for three gelation experiments to ensure reproducibility.

HCO is a heterogeneous material and degradation of this material is measured with bi-disperse MPT. HCO is supplied by Procter & Gamble Co. Briefly, HCO is made by dissolving the colloid at a concentration of 4 wt% into a 16 wt% linear alkylbenzene sulfonate solution. The solution is stirred at 300 rpm and heated to 92 °C for 5 min and then cooled at 55 °C. Setting the cooling temperature to 55 °C promotes a fibrous colloidal growth with aspect ratios ranging from 50–2500, and a corresponding fiber length of 1–50 μm.[39–41] Differential interference contrast imaging verifies that fibers account for 95% of the final colloid morphology.[7] HCO undergoes controlled degradation by inducing an osmotic pressure gradient. A 4 wt% HCO gel is contacted with water to induce degradation. The water reduces the attractive forces between the colloidal fibers, degrading the gel until it undergoes a phase transition and reaches a new equilibrium sol phase. These experiments are done in a sample chamber made in a 35 mm glass-bottomed petri dish (MatTek Corporation), constructed with 0.15 mm thick glass spacers, a glass coverslip (22 × 22 × 0.13–0.17 mm, Fisher Scientific) and UV curable adhesive (NOA-81, Norland Products Inc.).[7] Data are collected for three different HCO degradation experiments for reproducibility.

2.2 Multiple particle tracking microrheology

MPT is used to measure the rheological and material properties of soft matter. In MPT, fluorescently labeled probe particles are embedded in a sample and video microscopy is used to capture the particle movement or Brownian motion. MPT data are collected using a Zeiss Observer Z1 (Carl Zeiss AG) with a water immersion objective with a low numerical aperture (63×, N.A. 1.3, 1× optovar, Carl Zeiss AG). Videos are recorded on a Phantom Miro M10 high-speed camera (Vision Research, Inc.) at a resolution of 1024 × 1024 pixels, 30 frames per second frame rate, and 1000 μs exposure time. The equipment is calibrated to minimize static and dynamic particle tracking error of 0.5 μm probe particles.[4] These errors are discussed in detail below.

The brightness-weighted centroid of each probe particle is identified in each frame of the collected video using tracking algorithms developed by Crocker and Grier.[1] These probe particle positions are then linked together into trajectories. Particle positions are linked using the probability that a Brownian particle will diffuse a certain distance, which is dependent on the probe particle self-diffusion coefficient.[1] The ensemble-averaged mean-squared displacement (MSD, $\langle \Delta r^2(\tau) \rangle$) is then calculated from the particle trajectories in our two-dimensional measurements using $\langle \Delta r^2(\tau) \rangle = \langle \Delta x^2(\tau) \rangle + \langle \Delta y^2(\tau) \rangle$ where x and y are coordinates and τ is the lag time. The ensemble-averaged MSD is related to material properties, such as the creep compliance, using the GSER

$$\langle \Delta r^2(t) \rangle = \frac{k_B T}{\pi a} J(t) \quad (1)$$

where $J(t)$ is the creep compliance, $k_B T$ is the thermal energy and a is the particle radius.[1–4,15,42] Additionally, the MSD can be related to particle diffusivity, D, by $\langle \Delta r^2(\tau) \rangle = 2dD\tau^{\alpha}$ where d is the number of dimensions of the measurement, τ is the lag time and α is the logarithmic slope of the MSD, $\alpha = \frac{\mathrm{d} \log \langle \Delta r^2(\tau) \rangle}{\mathrm{d} \log \tau}$.[1–5,8–15]

An advantage of MPT is the sensitivity of the measurement, which is able to characterize the precise change in the state of the material, *i.e.* from a sol to a gel during gelation or a gel to a sol in degradation. To determine the state of the material we use the value of the logarithmic slope of the MSD, α.[7,9,26–28,36,43] $\alpha = 1$ indicates that probe particles are freely diffusing and the material is a sol. $\alpha \to 0$ measures no probe particle movement indicating that the material is a gel. With MPT we can also determine the precise time when the first sample-spanning network cluster forms in gelation or breaks in degradation. To define this critical transition, we first determine the critical relaxation exponent, n, using time-cure superposition.[44,45] This value is a measure of the structure of the gel, *i.e.* densely or loosely cross-linked, and also pinpoints the critical gel transition when $\alpha = n$.[7,26–28,36] This technique will be discussed in more detail in the Results & discussion section.

2.3 Bi-disperse multiple particle tracking

In conventional MPT, a single probe particle size is used to ensure that all assumptions of microrheology are met. Using a single particle enables design of experiments where the particle size is greater than the native length scale of the material, there are no particle–particle or particle–material interactions and probes are not settling due to gravity, which would limit the amount of measurable particle movement before it leaves the field-of-view.[24,46] Although a single particle size simplifies the design of experiments, there are distinct advantages to having more than one probe particle size to simultaneously measure different length scales of the material in a single sample. Using a bi-disperse probe radius distribution means that the normal methods of particle tracking must be modified to separate the two particles in each video. The particles are separated because the calculation of the rheological properties is dependent on the particle radius. To track both particle sizes, we have leveraged parameters that were already part of the particle tracking algorithms developed by John C. Crocker, David Grier and Eric R. Weeks (http://www.physics.emory.edu/~weeks/idl/index.html).[1,42] The individual particles of different sizes can be separated into two populations by using the squared radius of gyration, R_g^2, already calculated in the particle tracking algorithm. This squared radius of gyration is based on the brightness of pixels in an image,

$$R_g^2 = \frac{I}{B} \quad (2)$$

where I is the moment of inertia of an object and B is a "weight" represented by the summation of the brightness of each pixel in the particle. This is a general form of a squared radius of

gyration, and is widely applicable to different systems including those that define mass by brightness.[47] I is defined by

$$I = \sum \left(b_i \times \left(r_i^2 + \frac{1}{6} \right) \right) \quad (3)$$

where b_i is the brightness of a given pixel at a radius r_i away from the center of mass. The additional $\left(\frac{1}{6} \times b_i\right)$ term in the equation is added as the moment of inertia of a square prism with a length of 1 pixel.[42] R_g^2 is used in our work to separate particle sizes, as shown in Fig. 1a. The large separation is due to the r^2 term in eqn (3). This results in an increased value of R_g^2 by an increase in the amount of pixels the object appears in, even if the overall particle has a similar average brightness. It should be noted that there are deviations in Fig. 1a. The value of R_g^2 is calculated early in the tracking process and these deviations are due to identification of bright pixels that may not be particles. Additional filtering steps that include filtering for brightness, mass and eccentricity, are used to ensure only probe particles are tracked and are standard in MPT data analysis.[1]

Using this value of R_g^2 the different sized probe particles are separated into two distinct populations, one with $R_g^2 < 0.33$ μm^2 (0.5 μm probes) and another of $R_g^2 > 0.33$ μm^2 (2 μm probes). These ranges of R_g^2 are for this particular sample, and will change based on each experiment due to the amount of illumination of the probe particles. The separation value for the probe populations is determined by estimating the center of the distribution of R_g^2 for each particle size and calculating the mid-point between these values. This mid-point is then used as the separation value of R_g^2. The video is then tracked twice, tracking probes above or below the separation value of R_g^2 shown by the circled particles in Fig. 1b and c. The MSD is then calculated for each population separately. In the following sections we use a viscous Newtonian fluid to validate the technique and then show the sensitivity of the technique to different length scales in a homogeneous and heterogeneous gel system.

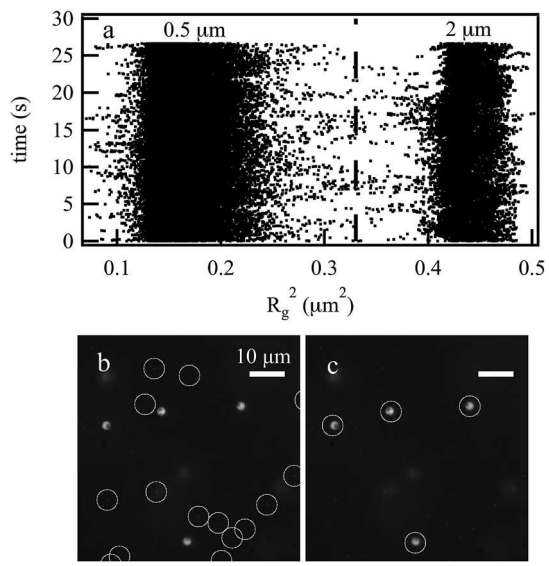

Fig. 1 (a) Individual probe particle squared radii of gyration with a separation cutoff of R_g^2 = 0.325 μm^2 (dashed vertical line). Fluorescent images of probe particles in a 5% glycerol solution with circled (b) 0.5 μm and (c) 2 μm probes.

2.4 Static and dynamic particle tracking errors

Using bi-disperse particles for MPT measurements can increase errors in the measurements, namely static and dynamic particle tracking errors. The analysis of static and dynamic particle tracking errors was first introduced by Savin and Doyle.[4] Static error is a function of the equipment used in microrheology experiments. This is an error in the ability of the apparatus to locate the exact position of the particle. The actual position of the static particle, $x(t)$, is offset by the recorded probe particle position, $\hat{x}(t)$, by the random error $\chi(t)$.[4,20] To correct for static error the following equation is used

$$\hat{x}(t) = x(t) + \chi(t). \quad (4)$$

Dynamic error is the error in identifying the precise position of the particle center when it is moving. If the exposure time is too long when capturing particle movement, the particle center will be the time-averaged center which will not be the precise particle location.[4,48] Static and dynamic error can be balanced by precisely calibrating the experimental apparatus to a chosen probe particle size. This is done by measuring Brownian probe particle movement with varying frame rates and exposure times. We characterize decreased particle diffusivity in a Newtonian fluid by increasing viscosity. These measurements are necessary for calibration because these errors change as probe particle movement decreases. These calibration experiments identify the frame rate and exposure time where static and dynamic error are minimized. Since the calibration is specific to a single particle size, using a bi-disperse particle population means that only one particle will have minimal static and dynamic error and the other particle size must have these errors accounted for after data acquisition.

For our measurements, our experimental apparatus is calibrated to minimize static and dynamic error for the 0.5 μm particles. Therefore, we must account for these errors only in the 2 μm particle data. Since 2 μm particles undergo slow diffusivity we do not measure a large amount of dynamic error in our samples. Instead static error dominates and is accounted for. The presence of static error in the 2 μm particle data is apparent in the calculated subdiffusive movement which results in the decreased logarithmic slope of the MSD, α, at short lag times.

The value of random error, $\chi(t)$, is determined by recording probe particles that are not moving, such as in a gel or settled on a surface. For our measurements, we force probes to settle on a coverslip to restrict movement. 2 μm probes are diluted with a 1 M NaCl solution to a final concentration of 0.0025% solids per volume. Probes crash out of solution overnight. MPT data are collected and tracked. The MSD of these particles is calculated, Fig. S1 (ESI†), to determine the value of $\chi(\tau)$. This is a constant value at all lag times. The value for static error for 2 μm particles in this experimental apparatus is $\chi = 2.0 \times 10^{-3}$ μm^2.

This value is subtracted from the calculated MSDs for all 2 μm probe particle measurements.

3 Results & discussion

3.1 Validation with glycerol viscosity measurements

The viscosity of glycerol, a Newtonian fluid, at varying concentrations is measured with MPT using bi-disperse probe particles sizes, Fig. 2. Fig. 2a are MSDs measured with 0.5 and 2 μm probe particles for 0 wt% and 40 wt% glycerol. The shape of the MSD curves are indicative of a Newtonian fluid. At all concentrations and for both probe sizes $\alpha = 1$ for the entire MSD curve, indicating Brownian diffusion of the particles. The magnitude of the MSDs decreases for increasing concentration and probe particle diameter. A decrease in the magnitude of the MSDs when glycerol concentration is increased indicates an increase in viscosity and a decrease in particle diffusion. The magnitude of the MSDs also decreases when the probe particle size is increased in the same glycerol concentration. This indicates that smaller probe particles have greater diffusivity in the same solution.

Fig. 2b shows calculations of the viscosity of glycerol solutions at varying concentrations. The viscosity, η, is calculated for each sample using

$$\eta = \frac{k_B T}{6\pi a D} \quad (5)$$

where $k_B T$ is the thermal energy, a is probe radius and D is the diffusivity determined from the MSDs.[1–3,15] Measurements from bi-disperse MPT experiments are graphed with tabulated data at 25 °C.[34] As shown from Fig. 2b, the calculated viscosities for both particles match well with the tabulated values of viscosity. This indicates that the addition of a second particle size to our MPT measurements has not adversely affected the measurements. Instead both particle sizes are measuring the same viscosity in the samples and that viscosity is consistent with independent measurements. This validates the technique. To further illustrate the capabilities of this technique we measure gelation of a homogeneous PEG-acrylate:PEG-dithiol hydrogel scaffold and a heterogeneous hydrogenated castor oil colloidal gel network.

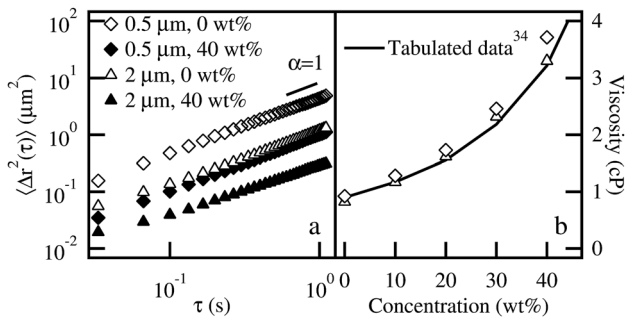

Fig. 2 Glycerol dilution measured with bi-disperse MPT. (a) Mean-squared displacement curves for bi-disperse probe particles in 0 and 40 wt% glycerol solutions. (b) Viscosity of glycerol at various concentrations calculated from 0.5 μm and 2 μm probes using bi-disperse MPT in the same sample, which is compared to previously reported values.[34]

3.2 Characterization of homogeneous PEG-acrylate:PEG-dithiol gelation

The next experiments focus on characterizing the gelation of a homogeneous chemically cross-linked polymeric hydrogel. MPT measures the change in rheological properties from polymer solution (18 wt% PEG-acrylate, 3.8 wt% PEG-dithiol) to a cross-linked hydrogel scaffold by increasing exposure to UV light.[36] We chose to characterize this hydrogel scaffold with the starting polymeric solution in the semi-dilute regime. A solution is in the semi-dilute regime when the concentration is greater than the overlap concentration, c^*, but less than the entanglement concentration, c^{**}, $c^* < c < c^{**}$. The overlap concentration for the backbone PEG-acrylate molecule is $c^* = 0.13 \pm 0.04$ g mL^{-1}.[36] In the semi-dilute region, the viscosity of the polymeric solution increases with concentration as $\log\eta \propto 2\log c$ due to polymeric interactions.[36,49] This system is characterized in the semi-dilute regime because the relatively higher viscosity of the precursor solution further limits the amount of 2 μm probes settling during experimental setup.

Fig. 3 shows microrheology results for the PEG-acrylate:PEG-dithiol chain-growth gelation reaction. This hydrogel system gels when exposed to UV light. After each UV exposure, MPT data are collected to determine the rheological properties. The MSD curves, Fig. 3a and b, show the change in rheological properties during the gelation reaction for both particle sizes. The magnitude and logarithmic slope of the MSD, α, decrease as the extent of reaction increases and the material transitions from a sol to a gel. This is also shown in the α values of the individual MSDs, Fig. 3c. The results from bi-disperse MPT measurements agree well with previous measurements using 1 μm particles.[36] With UV exposure there is no change in the MSD magnitude or α as radicals build up in the system and polymer chains form. Then the MSD and α values decrease rapidly as gelation occurs at 28 min. Several observations can be made when using different probe particles sizes. Gelation is measured with both particle sizes, as can be seen from the rapid decrease in α at 28 min in Fig. 3c. Even though both probe particles are sensitive to gelation on the same time scale, there are differences in the MSD curves prior to gelation. The expected value of α is measured for the 0.5 μm particles, $\alpha \approx 1$. The 2 μm probe particles have lower α values, between approximately $0.6 < \alpha < 0.8$. The lower value of α prior to gelation is most likely due to the 2 μm probes measuring viscoelastic properties of the precursor solution.[15]

Fig. 3d is the non-Gaussian parameter, α_{NG}, for both particle sizes. The non-Gaussian parameter is defined as $\alpha_{NG} = \frac{\langle \Delta x^4 \rangle}{3\langle \Delta x^2 \rangle^2} - 1$. α_{NG} is calculated to determine the heterogeneity in the system.[36,50–52] This value represents the deviation of the 1-dimensional probe particle displacement from Gaussian-like behavior, with a larger value indicating a greater degree of heterogeneity. Previous work, determined that a PEG-acrylate:PEG-dithiol gelation was homogeneous when

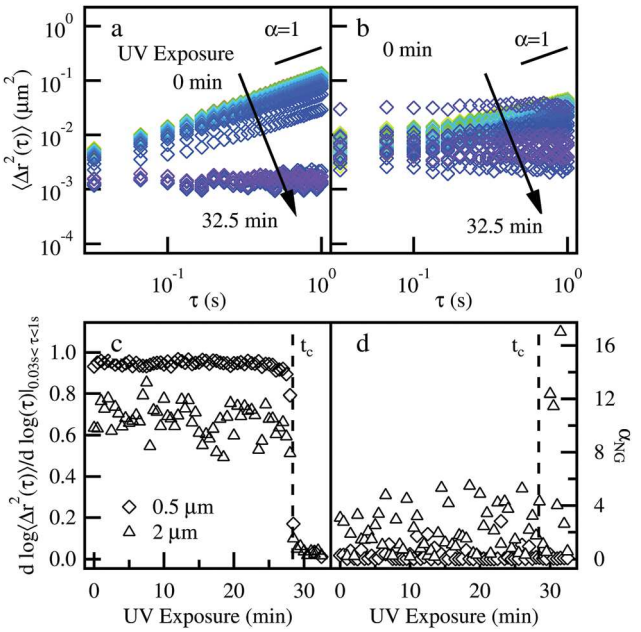

Fig. 3 Microrheology results for a PEG-acrylate:PEG-dithiol gelation. Gelation is induced by repeated exposure to UV light. Mean-squared displacement curves throughout the gelation for (a) 0.5 μm and (b) 2 μm probe particles. The color of the lines indicates UV exposure time and is consistent for (a and b). (c) Corresponding logarithmic slopes of the MSD (α) for the bi-disperse particle population. (d) Non-Gaussian parameter, α_{NG}, throughout the gelation reaction.

measured with a 1 μm probe particle.[36] This agreed with work by Tibbitt *et al.*, that determined chain-growth gelation reactions result in more homogeneous networks than step-growth gelation reactions.[53] In bi-disperse MPT, there is very little heterogeneity in the 0.5 μm particle displacements, and a larger overall value for the 2 μm displacements. Directly after gelation, where diffusivity of both probe particles is decreasing due to the formation of the network structure, there is a large increase in heterogeneity that is only measured in the 2 μm particle displacements. This occurs at the gel point and is due to an increase in entropy when the first sample-spanning network structure forms. When this first sample-spanning network cluster forms, large chains of polymers are cross-linking. This will lead to the largest porosity in the gel system, which has a heterogeneous microstructure and can only be measured by the 2 μm probes. This is also seen in Fig. 3b for the 2 μm particles. There is an increase in the magnitude of the MSD when heterogeneity or α_{NG} is at a maximum. This increase in MSD occurs in all experiments and is indicative of the large pore structure probed by these particles. After the sol–gel transition, the value of α_{NG} returns to the value measured prior to the critical transition. Using bi-disperse MPT, we are able to increase the amount of information about our hydrogel scaffold by quantifying large scale heterogeneities that would be unmeasurable if only small probes were used to measure this system.

To highlight the difference in the probe particle measurements in a single sample, we further investigate the difference in the MSD curves of the precursor solution prior to UV exposure, Fig. 4a. From the MSD curves, there is a distinct difference between the measurement of the two particle sizes. The 0.5 μm particles only measure Brownian motion of the probes indicating that there is no polymeric interactions or viscoelastic properties in this solution. The 2 μm probes have a decrease in α at the lowest lag times. This indicates that the probe particles are measuring viscoelastic properties due to the polymeric interactions in solution.[15] In the precursor solution, there are polymeric interactions of the PEG-acrylate backbone and linear PEG-dithiol cross-linker, which is at a concentration below c^*. These two polymers in solution lead to a mix of polymeric interactions and viscoelastic properties which are measured with bi-disperse MPT. The MSD curves are scaled by a factor of $\frac{\pi a}{k_B T}$, which shifts them by the particle size and the two curves overlay, Fig. 4b.[15] The scaled MSD values are an inverse modulus, or creep compliance.[15] At lower lag times, the curvature in the 2 μm probe particle measurements is due to sub-diffusive motion. At longer lag times, the 2 μm probe particles are measuring Brownian motion. This decrease at short lag times in polymer motion is a measure of the viscoelasticity in the sample and can be attributed to the relaxation time of the polymers in solution.[15] This is not measured with the 0.5 μm probe particles.

Time-cure superposition (TCS) is used to determine the gel point and critical relaxation exponent, n, for the PEG-acrylate: PEG-dithiol gelation, Fig. 5. TCS is an analysis technique which superimposes viscoelastic functions at different extents of gelation.[7–9,23,25,28,43–45,54] The gel point is defined as the time at which the first sample-spanning cluster is formed, t_c. For this reaction, extent of reaction, p, is assumed to be proportional to UV exposure time, t, as $p \propto t$. The MSDs are shifted into gel and sol master curves by a time shift factor, a, and a MSD shift factor, b, Fig. 5. The MSDs can be shifted because the relaxation of the polymers in the sol and network in the gel are measured in the shortest lag times and these relaxations are superimposed to form master curves.[7–9,23,25,28,43–45,54] Each shift factor

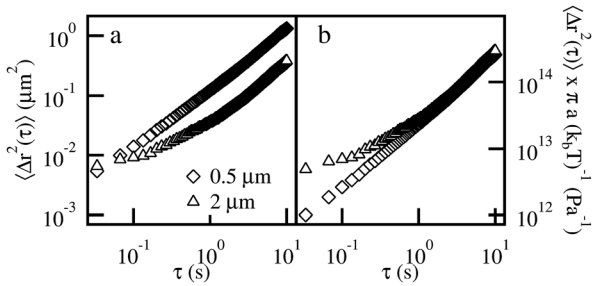

Fig. 4 Bi-disperse MPT of the PEG-acrylate:PEG-dithiol precursor solution prior to UV exposure. (a) MSDs of the PEG precursor solution which has polymeric interactions because the concentration is above the overlap concentration. The shape of the MSD curves differ at the shortest lag times. (b) The inverse modulus calculated by scaling the MSDs by the probe radius for both particles. The 0.5 μm particles measure only Brownian motion but the 2 μm particles are measuring viscoelasticity due to the relaxation of the polymers in solution.

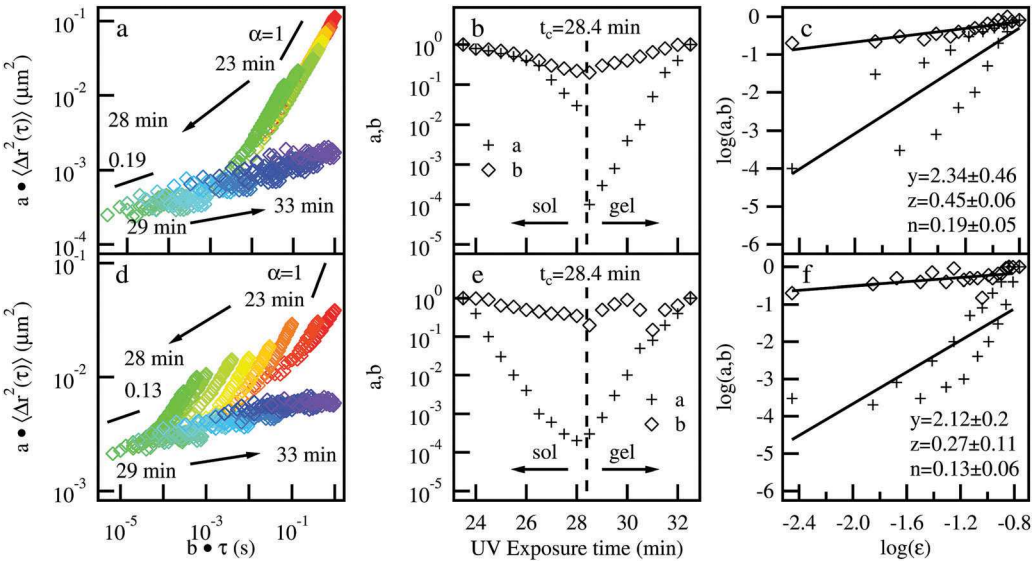

Fig. 5 Time-cure superposition of a PEG-acrylate:PEG-dithiol gelation reaction using bi-disperse MPT with (top row) 0.5 μm probes and (bottom row) 2 μm probes. (a and d) MSD curves shifted on the lag time and MSD axes to form sol and gel master curves. The unshifted MSD curves are shown in Fig. 3. (b and e) Shift factors *a* and *b* diverge at the critical gel point, t_c. (c and f) The values of *a* and *b* (using the same symbols from b and e) are used to calculate *y* and *z*, respectively. The error in the fit for *y* and *z* is the standard deviation. The critical relaxation exponent, *n*, is calculated from $n = \frac{z}{y}$.

determines a scaling exponent, which is then used to determine the critical relaxation exponent, *n*. The scaling exponents are related to the shift factors by the distance away from the critical extent of reaction defined as $\varepsilon = \frac{|t - t_c|}{t_c}$. The time shift factor, *a*, relates the longest relaxation time, τ_L, to the distance away from the critical extent of reaction by a scaling exponent, *y*, where $a \sim {\tau_L}^{-1} \sim \varepsilon^y$. The MSD shift factor, *b*, relates the steady state creep compliance, $J_{e,0}$, to the distance away from the critical extent of gelation by a scaling exponent, *z* using $b \sim {J_{e,0}}^{-1} \sim \varepsilon^z$.[7–9,23,25,28,45,54] The scaling exponents are then used to calculate the critical relaxation exponent, $n = \frac{z}{y}$.

The critical relaxation exponent, *n*, is a measure of the gel structure at the critical transition. *n* also determines how much energy the scaffold is likely to store or dissipate. In this way *n* is similar to a complex modulus. $n < 0.5$ indicates a densely cross-linked system that will readily store energy, while $n > 0.5$ indicates the gel is an open porous structure and will more likely dissipate energy. Previous MPT characterization of this gel using 1 μm probe particles determined $n = 0.13 \pm 0.01$.[36] This is a tightly cross-linked gel that will store energy.

Fig. 5 shows TCS for the PEG-acrylate:PEG-dithiol gelation reaction measured with bi-disperse MPT. Shifted MSD curves, Fig. 5a and d, for both particle sizes show a similar value of α at the sol–gel transition. It should also be noted that the shifted curves are not as smooth for the 2 μm probes. This is due to the measurement of the relaxation time of the polymers which causes a change in slope between short and long lag times. The shortest lag times are shifted to create the master curves, therefore, the change in slope does not adversely affect data analysis using TCS. The shift factors are plotted *versus* the UV exposure time, Fig. 5b and e. These graphs show the divergence of the shift factors at the gel point, t_c = 28.4 min. The gel point is the same for both probe particle sizes. Both probes measure the same gel point because they are both measuring the formation of a sample-spanning network cluster that has a native length scale that is smaller than both particle sizes. Finally, *n* is calculated from the scaling exponents *y* and *z*, with $n_{0.5\mu m} = 0.19 \pm 0.05$, and $n_{2\mu m} = 0.13 \pm 0.06$, Fig. 5c and f. As expected, these values are within error of each other and the previously reported value. From this analysis, we determine that both probe particle sizes accurately measure the gel point and critical relaxation exponent of this gelation reaction and using both particles gives further information about polymer relaxation and heterogeneity.

3.3 Characterization of heterogeneous hydrogenated castor oil degradation

Finally, degradation of a 4 wt% HCO fibrous colloidal gel is measured using bi-disperse probe particles, Fig. 6. This material has been previously characterized using only 0.5 μm particles.[6,7,37] In our previous characterization, we determined that the material evolves heterogeneously, with probe particle movement within a field-of-view ranging from Brownian motion to arrested within the gel network or clusters of fibers.[6,7,37] To illustrate that bi-disperse MPT can quantify material properties and provide additional information about the evolution of different length scales of structures we characterize HCO degradation. HCO degradation occurs when the colloidal gel is contacted with water which causes a decrease in the attractive forces between the colloids. Once the attractive forces weaken, water enters the gel and dilutes the colloids causing scaffold degradation. As the material degrades, the magnitude of the MSD curves and α values begin to increase, Fig. 6a and c. At the phase transition there is no longer a sample-spanning network of

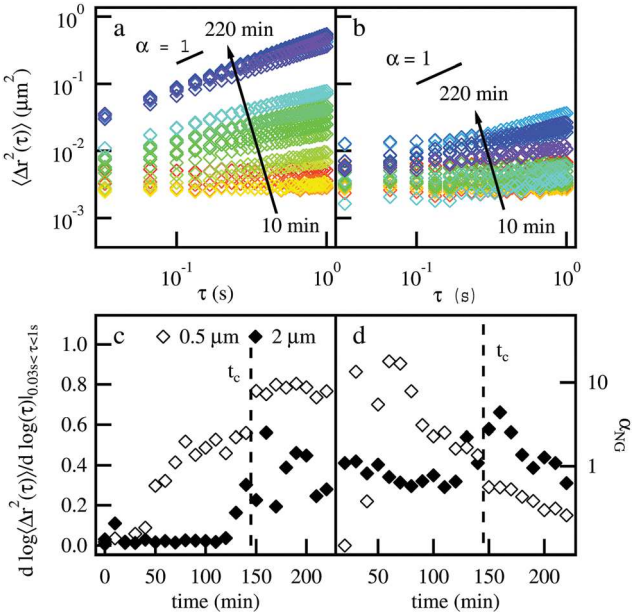

Fig. 6 Bi-disperse MPT measurements of the degradation of HCO induced by contacting the gel in water. Mean-squared displacement curves throughout the degradation for (a) 0.5 μm and (b) 2 μm probe particle sizes. (c) Corresponding logarithmic slopes of the MSD (α) and the (d) non-Gaussian parameter, α_{NG}, throughout degradation. Vertical dotted lines in (c and d) indicate the phase transition.

colloidal fibers and the material evolves to an equilibrated sol state. Similar to the PEG-acrylate:PEG-dithiol degradation, the 0.5 μm particles measure a greater particle motion at the end of the experiment, $\alpha \approx 0.8$, while the 2 μm particles have more restricted motion, $\alpha \approx 0.6$.

In comparison to previous work using just 0.5 μm particles, the rheological properties throughout degradation and the critical values at the phase transition measured with the 0.5 μm particles in bi-disperse MPT agree well.[6,7,37] An equilibrium phase with a corresponding $\alpha \approx 0.8$ is obtained. Using TCS, we determine that the phase transition occurs when $\alpha = n = 0.72 \pm 0.08$ at 144 min, Fig. S2a–c (ESI†).[7] In the same sample, degradation is measured at a different length scale with the 2 μm probes, Fig. 6b and c. The MSD curves and α values during the degradation do not increase as much as the 0.5 μm probes, and α remains at 0 for much longer. This is due to a larger structures remaining in the material that is being probed by the 2 μm particles and goes undetected by the 0.5 μm probes. After 2 hrs, α begins to increase, but the corresponding α values range between $0.2 < \alpha < 0.6$. Using TCS, we determine that the critical relaxation exponent is different for the degradation measured by 2 μm probes and is $n = 0.09 \pm 0.05$, Fig. S2d–f (ESI†). Although the value of n changes between the two measurements, the critical degradation time, t_c is similar. The critical degradation time does not change because this is the time when the material transitions from a gel to a sol. At this time the elastic moduli in the gel goes to 0 ($G' \rightarrow 0$) and the viscosity in the sol starts to increase.[7–9,23,25,28,43–45,54] These material properties would not be sensitive to the length scale of measurement and will be the same regardless of probe particle size.

The change in the value of n means that the 2 μm particles are probing a larger structure, which is a network of tightly associated HCO fibers. This can also be explained by considering the size of the fibers. HCO fibers are 20 nm in diameter and range from 1–50 μm in length.[7] We expect that due to the larger length of the HCO fibers there can be entanglements on the micron length scales that cannot be detected by the smaller probe particles. With a heterogeneous system, using a single particle size limits the measurement of the microenvironment. But repeating the experiment with different size particles can also provide conflicting information since heterogeneity evolves uniquely within each scaffold. This necessitates the use of bi-disperse particles to fully characterize the system.

The non-Gaussian parameter, α_{NG}, is also calculated for HCO degradation, shown here on a logarithmic scale to highlight changes between the probe particle sizes, Fig. 6d. The 0.5 μm probes show a maximum in the viscoelastic solid state during degradation and $\alpha_{NG} < 1$ in the equilibrium states. Again, this agrees with our previous measurements.[6,7,37] The 2 μm probes have a higher overall α_{NG} in the equilibrium states, $\alpha_{NG} \sim 1$. This trend of a higher overall value is similar to that measured in the PEG-acrylate:PEG-dithiol gelation reaction. Interestingly, when measured with 2 μm probes α_{NG} reaches a maximum at a different point in the gelation reaction. This maximum occurs at the phase transition and α_{NG} remains at its equilibrium value before and after the phase transition. This characterization determines that heterogeneity evolves over different time periods for the different length scales measured and suggests that at the gel point the porous structure is similar to the 2 μm length scale.

Rheological heterogeneity is also quantified for HCO degradation. An in-depth discussion of this analysis appears in the ESI.† In this analysis particles are clustered using an F-test with a 95% confidence interval of the variance of single particle van Hove correlation functions.[7,50–52] After the particles are clustered the MSD and diffusivity of the probes in each cluster is calculated. Using this analysis, we determine that the 0.5 μm particles in bi-disperse MPT agrees with previous measurements with the highest rheological heterogeneity occurring at a similar time as the maximum value of α_{NG}. Interestingly, we measure minimal changes in rheological heterogeneity with the 2 μm particles, because the diffusivity of most particles is close to the lower measurable limit of our experimental apparatus. In comparison to the 0.5 μm particles we would expect the diffusivity to be 4× lower in the 2 μm particles if we are measuring the same medium. But the diffusivity of the 0.5 μm particles is more than 4× greater than the diffusivity of the 2 μm particles. This indicates that the larger probes are measuring a different medium, which is most likely a larger length scale fibrous colloidal gel network. This conclusion is supported by Wilkins *et al.*, where they use confocal microscopy to relate rheological measurements to fibrous colloidal gel networks. In this work, they measure a fiber with a similar aspect ratio (polyamide).[55] They characterize the change in state of the material from an entangled network through a transitional phase to bundles of colloids in solution. Comparing these results, we determine that

the 2 μm probes are measuring a larger network structure that is likely in the transitional phase.[6,37,55]

4 Conclusions

This work shows that using bi-disperse MPT is a viable and valuable addition to multiple particle tracking microrheology for investigating the viscoelastic properties of soft materials. Data are collected using video microscopy of the bi-disperse particle population in the same sample. We have shown that there is a clear way to separate probe particles of different sizes in the same sample using existing particle tracking algorithms. The squared radius of gyration, R_g^2, is easily calculated and the particles with different radii can be separated using this value. Then each particle size is tracked separately and their mean-squared displacement is calculated.

We have also shown that the combination of particles does not interfere with the measurements of material properties, by validating the technique in glycerol, a Newtonian fluid. By systematic dilution of glycerol, we measure the material properties and determine that the viscosity measured from both probe particles agree with tabulated data. Homogeneous viscoelastic materials, such as the PEG-acrylate:PEG-dithiol hydrogel, also are accurately measured. We determine the critical gel time, t_c and the critical relaxation exponent, n, for the gelation of this scaffold using bi-disperse MPT. Both particles measure the same critical values. Additionally, the 2 μm particles are able to measure the relaxation in the precursor solution, which the 0.5 μm particles are not sensitive to. The technique also has clear advantages in measuring heterogeneous systems, which is illustrated with a heterogeneous HCO degradation. In these experiments, different particle sizes are able to measure different feature sizes within a single sample. This is evident in the quantification of heterogeneity in the scaffold, where the maximum heterogeneity is measured at two different times during the degradation reaction. This indicates that the heterogeneous structure evolves over different time and length scales during scaffold degradation.

This technique is not limited to the experimental systems discussed in this paper and can have important impact in the study of heterogeneous and biological materials, among others. In these systems feature sizes can vary in a small area and can be key to the function of the material. Measuring these materials using bi-disperse MPT will give additional information in a single sample, which can diminish number and cost of experiments and more completely characterize the system.

Conflicts of interest

There are no conflicts to declare.

Acknowledgements

The authors would like to acknowledge Han Zhang, Danielle Rafanelli, Shiqin He and John McGlynn for collection of preliminary data and help in developing this work. Funding for this work was provided by the Procter & Gamble Co. and the National Science Foundation under grant CBET-1751057.

References

1 J. C. Crocker and D. G. Grier, *J. Colloid Interface Sci.*, 1996, **179**, 298–310.
2 T. G. Mason, K. Ganesan, J. H. van Zanten, D. Wirtz and S. C. Kuo, *Phys. Rev. Lett.*, 1997, **79**, 3282–3285.
3 T. G. Mason, *Rheol. Acta*, 2000, **39**, 371–378.
4 T. Savin and P. S. Doyle, *Biophys. J.*, 2005, **88**, 623–638.
5 M. Caggioni, P. T. Spicer, D. L. Blair, S. E. Lindberg and D. A. Weitz, *J. Rheol.*, 2007, **51**, 851–865.
6 M. D. Wehrman, S. Lindberg and K. M. Schultz, *J. Rheol.*, 2018, **62**, 437–446.
7 M. D. Wehrman, S. Lindberg and K. M. Schultz, *Soft Matter*, 2016, **12**, 6463–6472.
8 A. M. Corrigan and A. M. Donald, *Langmuir*, 2009, **25**, 8599–8605.
9 A. M. Corrigan and A. M. Donald, *Eur. Phys. J. E: Soft Matter Biol. Phys.*, 2009, **28**, 457–462.
10 A. J. Levine and T. C. Lubensky, *Phys. Rev. Lett.*, 2000, **85**, 1774–1777.
11 T. H. Larsen, PhD thesis, University of Delaware, 2008.
12 B. R. Dasgupta, S. Tee, J. C. Crocker, B. J. Frisken and D. A. Weitz, *Phys. Rev. E: Stat., Nonlinear, Soft Matter Phys.*, 2002, **65**, 051505.
13 M. L. Gardel, M. T. Valentine, J. C. Crocker, A. R. Bausch and D. A. Weitz, *Phys. Rev. Lett.*, 2003, **91**, 158302.
14 T. A. Waigh, *Rep. Prog. Phys.*, 2005, **68**, 685–742.
15 E. M. Furst and T. M. Squires, *Microrheology*, Oxford University Press, 2017.
16 M. T. Valentine, P. D. Kaplan, J. C. Crocker, T. Gisler, R. K. Prud'homme, M. Beck and D. A. Weitz, *Phys. Rev. E: Stat., Nonlinear, Soft Matter Phys.*, 2001, **64**, 061506.
17 Q. Lu and M. J. Solomon, *Phys. Rev. E: Stat., Nonlinear, Soft Matter Phys.*, 2002, **66**, 061504.
18 J. Liu, M. Gardel, K. Kroy, E. Frey and B. D. Hoffman, *Phys. Rev. Lett.*, 2006, **96**, 118104.
19 R. Pandey and J. C. Conrad, *Phys. Rev. E*, 2016, **93**, 012610.
20 L.-C. Cheng, L. C. Hsiao and P. S. Doyle, *Soft Matter*, 2017, **13**, 6606.
21 T. Moschakis, B. S. Murray and E. Dickinson, *Langmuir*, 2006, **22**, 4710–4719.
22 J. P. Rich, G. McKinley and P. S. Doyle, *J. Rheol.*, 2011, **55**, 273–299.
23 K. M. Schultz, A. D. Baldwin, K. L. Kiick and E. M. Furst, *ACS Macro Lett.*, 2012, **1**, 706–708.
24 T. M. Squires and T. G. Mason, *Annu. Rev. Fluid Mech.*, 2010, **42**, 413–438.
25 T. H. Larsen and E. M. Furst, *Phys. Rev. Lett.*, 2008, **100**, 146001.
26 K. M. Schultz, A. D. Baldwin, K. L. Kiick and E. M. Furst, *Soft Matter*, 2009, **5**, 740–742.

27 T. H. Larsen, M. C. Branco, K. Rajagopal, J. P. Schneider and E. M. Furst, *Macromolecules*, 2009, **42**, 8443–8450.
28 K. M. Schultz and E. M. Furst, *Soft Matter*, 2012, **8**, 6198–6205.
29 M. T. Valentine, Z. E. Perlman, M. L. Gardel, J. H. Shin, P. Matsudaira, T. J. Mitchison and D. A. Weitz, *Biophys. J.*, 2004, **86**, 4004–4014.
30 N. J. Hoh and R. N. Zia, *Lab Chip*, 2016, **16**, 3114–3129.
31 I. Sriram, A. Meyer and E. M. Furst, *Phys. Fluids*, 2010, **22**, 062003.
32 I. Sriram, R. J. DePuit, T. M. Squires and E. M. Furst, *J. Rheol.*, 2009, **53**, 1–30.
33 S. C. Chew, B. Kundukad, T. Seviour, J. R. C. van der Maarel, L. Yang, S. A. Rice, P. S. Doyle and S. Kjelleberg, *mBio*, 2014, **5**, e01536.
34 D. C. Company, *Online publication*, 2011.
35 K. M. Schultz and E. M. Furst, *Lab Chip*, 2011, **11**, 3802–3809.
36 M. D. Wehrman, A. Leduc, H. E. Callahan, M. S. Mazzeo, M. Schumm and K. M. Schultz, *AIChE J.*, 2018, DOI: 10.1002/aic.16062.
37 M. D. Wehrman, M. J. Milstrey, S. Lindberg and K. M. Schultz, *Lab Chip*, 2017, **17**, 2085–2094.
38 B. D. Fairbanks, M. P. Schwartz, C. N. Bowman and K. S. Anseth, *Biomaterials*, 2009, **30**, 6702–6707.
39 D. Yang and A. N. Hrymak, *Ind. Eng. Chem. Res.*, 2011, **50**, 11585–11593.
40 D. Yang, A. N. Hrymak and M. R. Kamal, *Ind. Eng. Chem. Res.*, 2011, **50**, 11594–11600.
41 N. D. Meirleir, L. Pellens, W. Broeckx, G. van Assche and W. D. Malshe, *Colloid Polym. Sci.*, 2014, **292**, 2539–2547.
42 J. C. Crocker and E. R. Weeks, 2011, http://www.physics.emory.edu/~weeks/idl/index.html.
43 D. Stauffer, A. Coniglio and M. Adam, *Adv. Polym. Sci.*, 1982, **44**, 103–158.
44 H. H. Winter and F. Chambon, *J. Rheol.*, 1986, **30**, 367–382.
45 D. Adolf and J. E. Martin, *Macromolecules*, 1990, **23**, 3700–3704.
46 D. T. Chen, E. R. Weeks, J. C. Crocker, M. F. Islam, R. Verma, J. Gruber, A. J. Levine, T. C. Tubensky and A. G. Yodh, *Phys. Rev. Lett.*, 2003, **90**, 108301.
47 H. Goldstein, *Classical Mechanics*, Addison-Wesley, 1950.
48 J. C. Crocker and B. D. Hoffman, *Methods Cell Biol.*, 2007, **83**, 141–178.
49 M. Rubinstein and R. H. Colby, *Polymer Physics*, Oxford University Press, 1st edn, 2003.
50 A. Heuer and K. Okun, *J. Chem. Phys.*, 1997, **106**, 6176–6186.
51 A. Rahman, *Phys. Rev.*, 1964, **136**, 405–411.
52 J. C. Crocker, M. T. Valentine, E. R. Weeks, T. Gisler, P. D. Kaplan, A. G. Yodh and D. A. Weitz, *Phys. Rev. Lett.*, 2000, **85**, 888–891.
53 M. W. Tibbitt, A. M. Kloxin, L. Sawicki and K. S. Anseth, *Macromolecules*, 2013, **46**, 2785–2792.
54 K. M. Schultz, A. D. Baldwin, K. L. Kiick and E. M. Furst, *Macromolecules*, 2009, **42**, 5310–5316.
55 G. M. H. Wilkins, P. T. Spicer and M. J. Solomon, *Langmuir*, 2009, **25**, 8951–8959.

